



Conference Proceedings Paper – Remote Sensing

Using Giovanni with Tri-Plot to Create a Simple Ternary Optical Classification System for Ocean Surface Waters

James Acker^{1*}, and Erik Douds^{2†}

¹ NASA Goddard Earth Sciences Data and Information Services Center, Code 610. 2, NASA Goddard Space Flight Center, Greenbelt, MD, 20771 USA; james.g.acker@nasa.gov.

² Colby College, eadouds@gmail.com.

† These authors contributed equally to this work.

* Author to whom correspondence should be addressed; E-Mail: james.g.acker@nasa.gov; Tel.: +1-301-614-5435 (ext. 123).

Published: 25 June 2015

Abstract:

We have devised a simple optical parameter classification system using three inherent optical property (IOP) parameters available in the NASA Geospatial Interactive Online Visualization and Analysis Infrastructure (Giovanni). These parameters are produced by the NASA Ocean Biology Processing Group (OBPG). The three IOP parameters are: a_{dg} , the absorption coefficient of dissolved and detrital matter; a_{ph} , the absorption coefficient of phytoplankton, and b_{bp} , the backscatter coefficient. The Microsoft Excel ternary diagram plotting spreadsheet *Tri-plot* (Graham and Midgely 2000) was used for visualization of the three-component ocean optical parameter classification scheme. In this paper we demonstrate this ternary optical classification system by examining the seasonal outflow of the Orinoco River into the eastern Caribbean Sea. End-member optical regimes consist of river mouth waters during the rainy season, and high clarity Caribbean Sea waters which are not influenced by the optically active constituents in the Orinoco River plume. Variability of the optical characteristics of surface waters between rainy and dry seasons is clearly distinguishable in the ternary plots, particularly in the coastal region adjacent to the northern coast of South America. This simple analysis method can be utilized by researchers, continuous water quality monitoring campaigns, citizen scientists, teachers, and students.

Keywords: Ocean optics, remote sensing, phytoplankton, organic matter, scattering, absorption

1. Introduction

The first description of optical water mass classification for oceanographic research is attributed to Jerlov (1). Jerlov's initial schema proposed three optical water mass classifications, which he later expanded to five, and in the course of this revision he also included nine different coastal water types. Jerlov used spectral diffuse attenuation coefficients for his initial classification method. (2, 3)

Subsequent to Jerlov's pioneering work, several different optical water mass classification methods have been developed. One of the most familiar and widely-used is the Case 1/Case 2 classification system of Morel and Prieur (4). In the Morel and Prieur system, Case 1 water is defined as water masses where the only influence on the optical properties is due to the optical properties of water and absorption or scattering by phytoplankton. Case 2 waters are waters in which the presence of any other dissolved or suspended constituent, such as organic matter, *Gelbstoff*, and terrestrial or marine sediments, influences the optical properties of the water mass. Pure occurrences of Case 1 waters are unusual, and are indicative of open-ocean conditions at a considerable distance from land. Case 2 waters exhibit optical complexity due to the potential presence of several different constituents which can determine their optical properties.

The use of remote-sensing data has allowed optical water mass classification to be performed on larger areas than is possible from shipboard measurements. Ocean color radiometric data products from the Sea-viewing Wide Field-of-view Sensor (SeaWiFS) and the Moderate Resolution Imaging Spectroradiometer (MODIS), available from the National Aeronautics and Space Administration (NASA), include optical property variables that can be utilized for water mass classification, in addition to the more familiar ocean color data variables, such as chlorophyll *a* concentration (chl *a*), the diffuse attenuation coefficient at 490 nm (K_{490}), or euphotic depth (Z_{eu}). Three optical property parameters that can be employed for optical water mass classification are the absorption coefficient of phytoplankton (a_{ph}), the absorption coefficient for dissolved and detrital material (a_{dg}), and the backscattering coefficient (b_{bp}). In this paper, a_{dg} and b_{bp} were generated by the "Garver-Siegel-Maritorena" (GSM) algorithm (5), and a_{ph} was generated by the Quasi Analytical Algorithm (QAA) of Lee et al. (6) The GSM data parameters were preferred over the QAA data products due to lesser noise in the QAA parameters. The method demonstrated here would also work with the QAA a_{dg} and b_{bp} parameters.

The absorption coefficient of phytoplankton (a_{ph}) is indicative of the presence of phytoplankton cells containing chlorophyll. The absorption coefficient for dissolved and detrital material (a_{dg}) indicates the presence of chromophoric dissolved organic material (CDOM) and detritus, i.e., photo-active non-living material. This material frequently consists of the remains of phytoplankton that contain phaeopigments. CDOM may be terrestrial in origin, from rivers containing tannins or other plant pigments, or can be due to dissolved organic matter derived from phytoplankton, as in the case of hurricane storm wakes where photo-active organic matter in subsurface waters is brought to the surface by mixing (7, 8). The backscattering coefficient (b_{bp}) indicates the scattering of light by inorganic particles, usually marine or terrestrial sediments. In areas with high sediment load and high CDOM, there is likely to be some correlation between a_{dg} and b_{bp} . This covariation does not invalidate the method, but it will affect the distribution of the points on the plots. This method can be employed easily with other ocean optical data variables, including remote-sensing reflectances.

Arnone, Wood, and Gould (9) included the use of a three-component optical water mass classification system consisting of absorption by detritus, CDOM, and chlorophyll for the Gulf of Mexico – Mississippi River region. This brief discussion included an optical water mass classification ternary diagram. Gould and Arnone (10) expands on that analysis, using the same three-component ternary diagram method, in an analysis of the Gulf of Mexico – Mississippi River region for the period March 19 – April 1, 2003. By combining a satellite ocean color climatology with an optical water mass classification scheme, Gould et al. (11) mapped likely areas of benthic hypoxia along the Louisiana coast.

Depiction of three-component systems using ternary diagrams is common for mineral analyses of solid solution minerals, such as feldspars, which can vary in the relative amounts of potassium, sodium, and calcium, or the mineral composition of rocks, as for shales. (12) It is also common for the depiction of particle size distribution analyses. Ternary diagrams are very useful to demonstrate the relationships between the components of a three-component system. A simple way to generate ternary diagrams is through the use of the Tri-plot Excel spreadsheet application. (13) By utilizing National Aeronautics and Space Administration (NASA) ocean optical parameter data in combination with Tri-plot, a method for optical water mass classification with ternary diagrams that can be performed with relative ease has been developed. This paper describes the methodology of the Tri-plot optical water mass classification analysis, and demonstrates the method with an analysis of the influence of the Orinoco River outflow on the eastern Caribbean Sea basin.

The seasonal variability of the Orinoco River outflow in the Caribbean Sea has been observed in ocean color imagery commencing with the Coastal Zone Color Scanner (CZCS) mission and continuing with the SeaWiFS and MODIS missions. Initial observations of increased CZCS pigment concentration in the outflow region during the wet (rainy) season led to a basic conceptual understanding of increased nutrient concentrations in the river outflow enhancing phytoplankton productivity in Caribbean Sea waters. The observations indicated that the influence of the Orinoco River outflow plume could extend as far as Puerto Rico and Hispaniola. Subsequent research with improved data from SeaWiFS and MODIS indicated that the understanding based on CZCS data was in fact inaccurate; the primary optical constituent in the river outflow was not phytoplankton chlorophyll, but rather CDOM. High concentrations of absorbing CDOM were indistinguishable from chlorophyll by the CZCS pigment algorithm, and CDOM remains problematic, as it is difficult to fully deconvolute light absorption by CDOM and light absorption by chlorophyll. The use of apparent optical properties (AOP) for absorption by CDOM and chlorophyll provides an improved method of distinguishing between the two absorbing constituents in seawater.

In this study, ternary diagrams created with Tri-plot are used to perform three-component optical water mass classification using a_{ph} , a_{dg} , and b_{bp} for the Orinoco River outflow region of the eastern Caribbean Sea. This demonstration study compares the analysis for the wet season of April 2003 – August 2003 to the dry season of September 2003 – March 2004.

2. Results and Discussion

The expansion of the region influenced by the Orinoco River outflow is shown in Figure 1, using the a_{dg} parameter. Figure 5 in the Experimental Section depicts the four regions used for the optical water mass classification analysis.

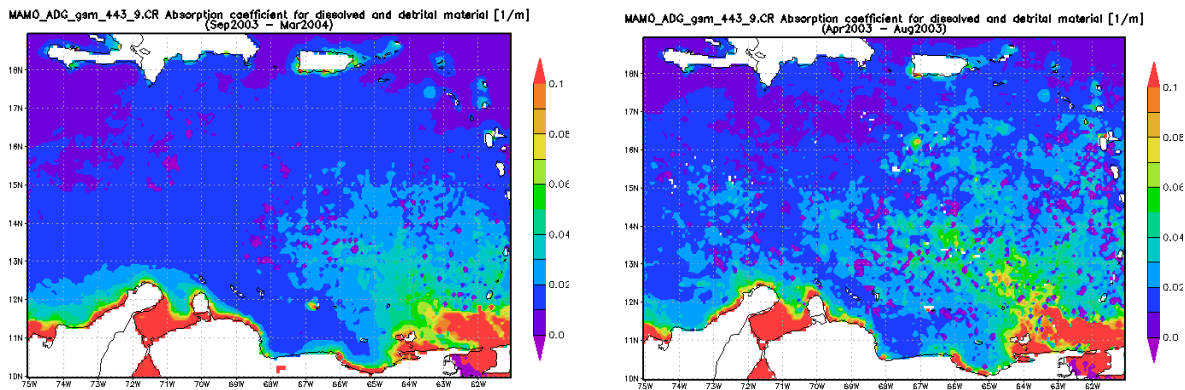


Figure 1. Monthly average maps of a_{dg} , showing the influence of the Orinoco River outflow on the Eastern Caribbean Sea Basin region. (left) Dry season, September 2003 – March 2004. (right) Wet season, April 2003 – August 2003.

In the following discussion, the Tri-plot ternary diagrams show the relative contributions of the three components of the optical water mass classification system as shown in Figure 2.

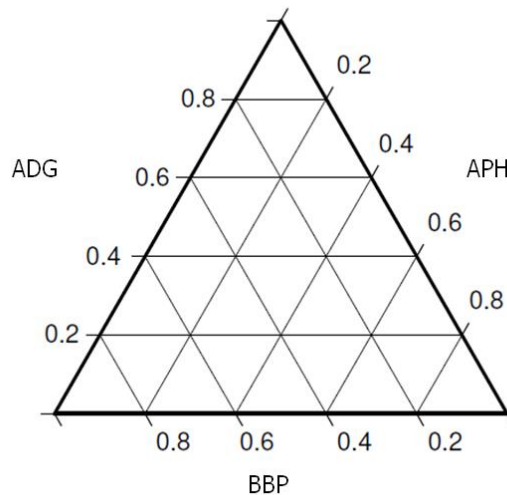


Figure 2. Ternary diagram for the three-component optical water mass classification system. ADG = absorption coefficient of CDOM and detritus; APH = absorption coefficient of phytoplankton; BBP = backscattering coefficient.

The first region to be examined is termed the Caribbean Sea Oligotrophic Waters (CSOW) region. Due to its distance from land and particularly from the Orinoco River outflow, this region

constitutes a clear-water, low-productivity end-member for the Caribbean Sea. Figure 3 compares the ternary plots for this region. In each of the following figures, the two ternary diagrams comparing wet versus dry season conditions have the same number of points; the difference in appearance results from changes in the data values, rather than extra observations. During the dry season, the points cluster toward the center of the ternary diagram, indicating a roughly equal contribution from all three optical components. During the wet season, we observe greater variability in the relative optical composition in this region (greater spread of the points on the ternary diagram), as well as a shift toward higher contribution by CDOM absorption, and thus a lower contribution by phytoplankton absorption and particle backscattering, represented by the shift in the distribution of points directly “up” in the ternary diagram.

Caribbean Sea Oligotrophic Waters (CSOW)

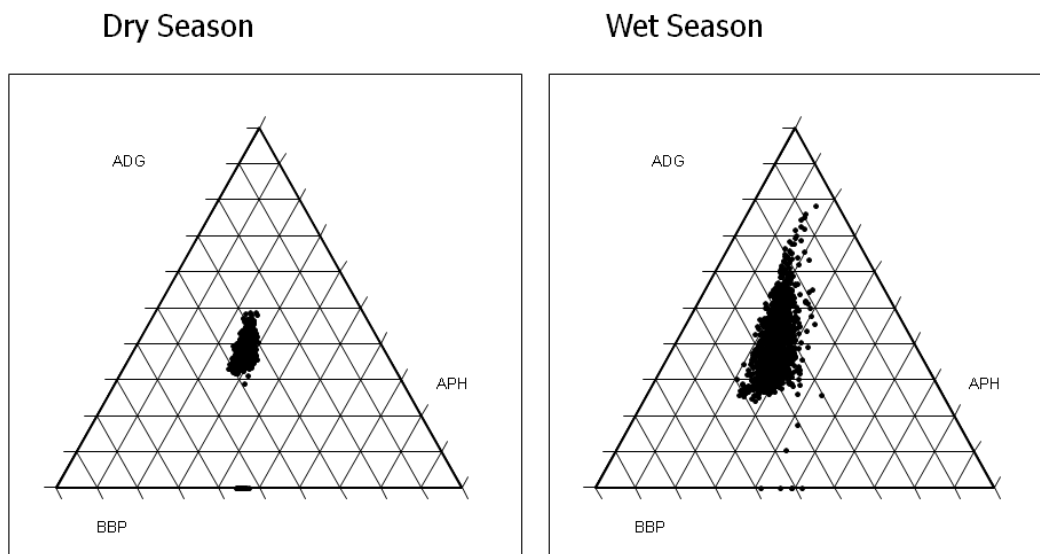
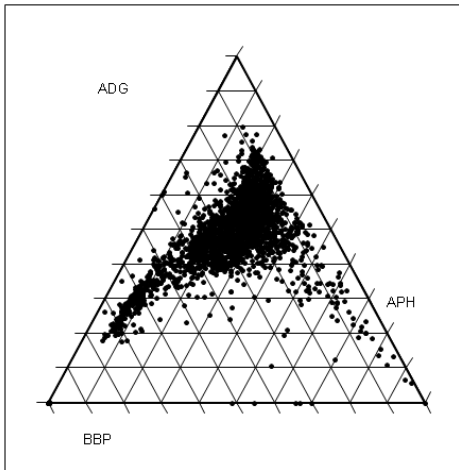


Figure 3. Ternary diagrams for the Caribbean Sea Oligotrophic Waters region during the dry and wet seasons. Each dot represents the calculated percentage contribution to the sum for each pixel in the area map of the region.

The next region examined is referred to as the Eastern Caribbean Basin region (Figure 4). Of note are in this diagram is the main conglomeration of points with elevated a_{dg} , and the two extensions into the high b_{bp} sector (lower left corner) and the high a_{ph} sector of the diagram (lower right corner).

Eastern Caribbean Basin

Dry Season



Wet Season

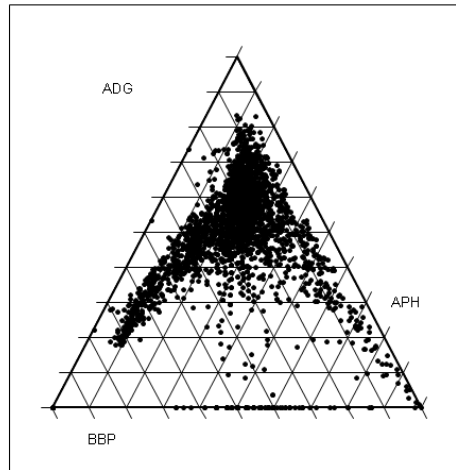
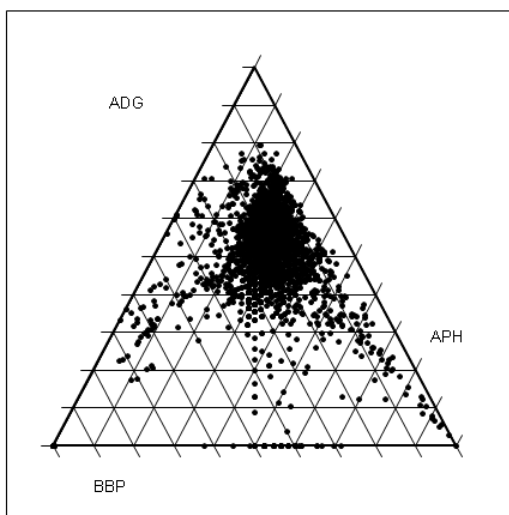


Figure 4. Ternary diagrams for the Eastern Caribbean Basin region during the dry and wet seasons.

Figure 5 provides the ternary diagrams for the region named “Orinoco River Plume”, and Figure 6 provides the ternary diagrams for the “Orinoco River Mouth” region. Note in Figure 5 that although most of the points are still located in the upper corner of the plot (indicating a relatively larger contribution from a_{dg}), we also observe an expansion of the main region of points downward and to the right in the ternary diagram. This indicates more points with a higher contribution from a_{ph} , and relatively lower contributions from a_{dg} and b_{bp} , particularly in the wet season.

Orinoco River Plume

Dry Season



Wet Season

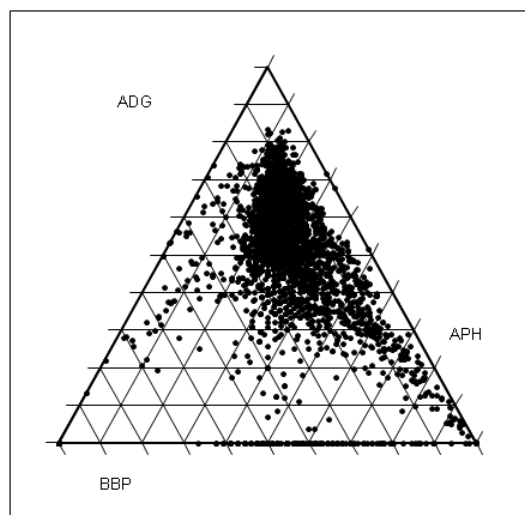
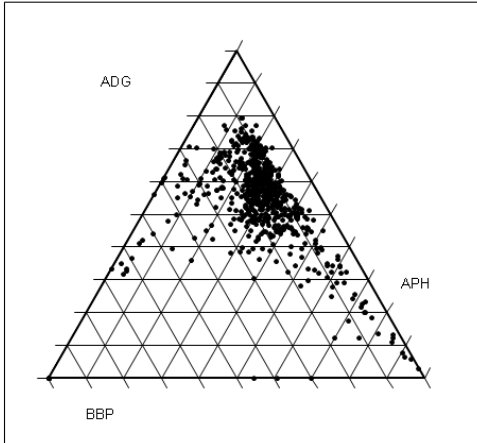


Figure 5. Ternary diagrams for the Eastern Caribbean Basin region during the dry and wet seasons.

Orinoco River Mouth

Dry Season



Wet Season

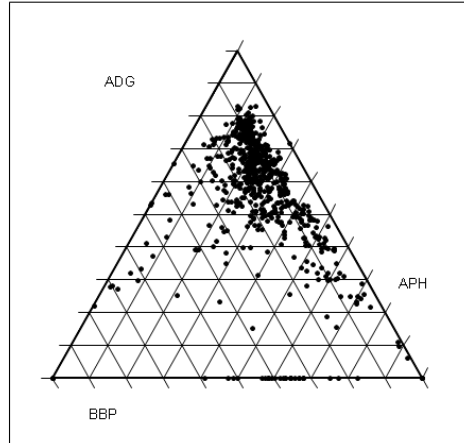


Figure 6. Ternary diagrams for the Orinoco River Mouth region during the dry and wet seasons.

Figure 6 indicates the primary optical signature of Orinoco River waters in the ternary diagram. Little difference is observed between the wet and dry seasons for this year (2003-2004).

Based on the ternary diagrams shown in Figures 3-6 for the selected regions in the eastern Caribbean Sea, it is possible using this system to identify four distinct optical water mass classes. These water mass classes are identified schematically in Figure 7 based on the dry season ternary diagrams. The *Caribbean Sea Oligotrophic Water* (CSOW) class has approximately 30% a_{ph} , 40% a_{dg} , and 30% b_{bp} . Note that in these very clear waters the values of all three IOPs are very low; the ternary diagram expresses the relative proportions of the three variables. The *Coastal* class exhibits high values of b_{bp} (due either to suspended coastal sediments or shallow bottom reflection) low values of a_{dg} , and very low values of a_{ph} . The *Case 1* class, based on the Morel and Prieur definition, has high values of a_{ph} and low values of b_{bp} and a_{dg} . The *Orinoco Plume* class has the highest values of a_{dg} , and low values of a_{ph} . Nearshore waters of the Orinoco Plume will have a higher contribution from b_{bp} .

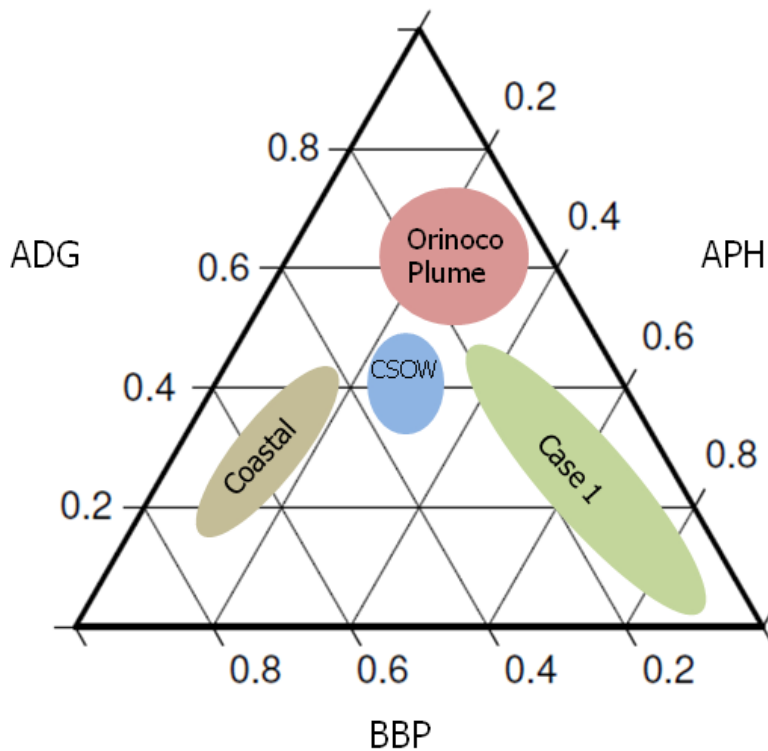


Figure 7. Four optical water mass classes, based on the ternary diagrams shown in Figures 3-6. The areas shown indicate the relative contribution of the three components of the optical water mass classification system. *Blue:* Caribbean Sea Oligotrophic Water class. *Tan:* Coastal Water class. *Green:* Case 1 Water class. *Magenta:* Orinoco Plume class.

The seasonal changes for this year observed in the ternary diagrams are depicted in Figure 8. The main change observed is the occurrence of more points that are designated for a fifth class, the *Wet Season Mixed* class. The main difference is a higher contribution from a_{ph} (40%) and lower contribution from a_{dg} (30%) with bbp similar to the CSOW (30%). This class encompasses a wide range of variability, as it includes the broad region where the rainy season flow of the Orinoco River is dispersed. Thus, the water mass represented by the Wet Season Mixed class results primarily from the mixing of CSOW with Orinoco Plume water. An additional factor is increased phytoplankton productivity in the mixed CSOW, due to higher nutrient concentrations in the Orinoco River outflow, which would contribute to higher values of a_{ph} . Note again in Figure 5, for the Orinoco Plume region, that there is an increased number of points in the Case 1 class during the wet season. Thus, even though the main regional effect of the Orinoco River outflow during the wet season on surface waters is an expansion of the spatial area where a_{dg} is elevated, there will still be an associated enhancement of phytoplankton productivity, evinced as elevated a_{ph} , due to terrestrially-derived nutrients in the river outflow.

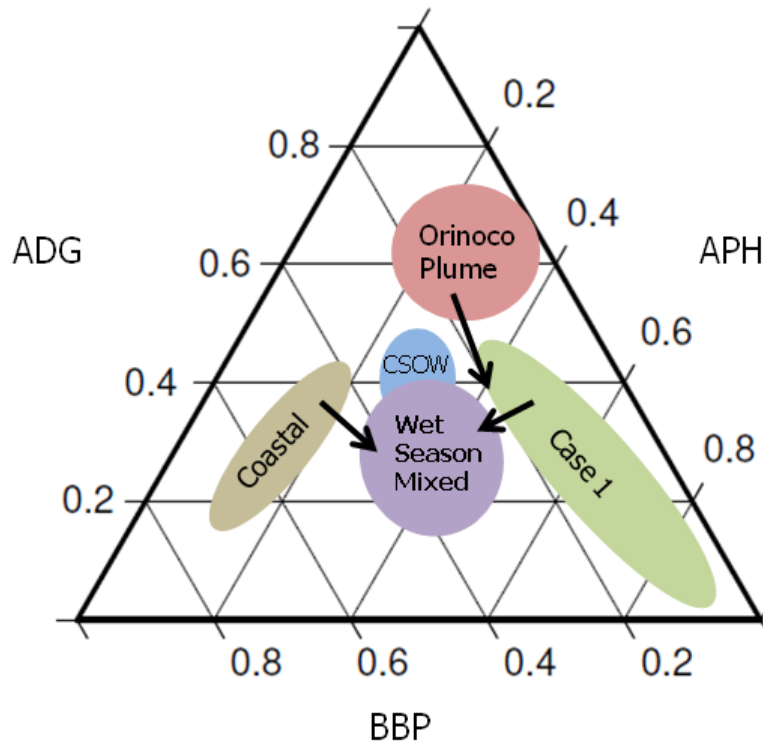


Figure 8. Changes in the optical water mass classes for wet season conditions. During the wet season, a group of pixels with a different contribution from the three components are distributed into an additional class, termed the *Wet Season Mixed* class.

3. Experimental Section

This study uses the National Aeronautics and Space Administration's (NASA) Geospatial Interactive Online Visualization ANd aNalysis System (Giovanni) and Tri-plot, an Excel spreadsheet application, to perform a three-component optical water mass classification. The three-component system generates ternary optical water mass diagrams. MODIS-Aqua satellite-based ocean color radiometric data are used exclusively in this example.

Our study focuses on the outflow region of the Orinoco River into the Caribbean Sea. The sample area has three spatial scales and two temporal scales to capture data on the various characteristics of the watershed.

This is the first publication describing the use of Giovanni and Triplot to download remotely-sensed optical properties, which are used to produce ternary plots for water quality analysis. Giovanni is comprised of a wide range of parameters, to meet the specific fields of Earth science. Therefore, the method used in this study could potentially be replicated and applied to other studies besides ocean optics, provided that a three-component system can be devised.

3.1. Data Acquisition

Area maps of the three water quality parameters a_{ph} , a_{dg} , and b_{bp} were generated by creating area maps of each parameter with Giovanni. The full data variable names of the three parameters we examined are “Absorption coefficient for dissolved and detrital material” (*MAMO_ADG_gsm_443_9.CR*), “Absorption coefficient for phytoplankton” (*MAMO_APH_gsm_443_9.CR*), and “Backscattering coefficient for particulate matter” (*MAMO_BBP_gsm_443_9.CR*). The monthly Level 3 MODIS-Aqua data products were utilized.

These three optical parameters were mapped for four different spatial scales to capture the full characteristics of the Orinoco River outflow region of the Caribbean Sea. These are termed “Eastern Caribbean Basin”, “Orinoco River Plume”, “Orinoco River Mouth”, and “Caribbean Sea Oligotrophic Waters”. Table 1 provides the exact latitude-longitude coordinates chosen for each of these areas. Figure 9 depicts the four regions using the a_{ph} parameter during the dry season. The white rectangle in the Eastern Caribbean Basin map is the Caribbean Sea Oligotrophic Waters region.

Table 1. Latitude-longitude corner points for the four spatial scales used in the analysis.

Eastern Caribbean Basin	Orinoco River Plume	Orinoco River Mouth	Caribbean Sea Oligotrophic Waters
West: -75	West: -67	West: -63	West: -74
North: 19	North: 14	North: 12	North: 17
South: 10	South: 9	South: 9.5	South: 15
East: -61	East: -60	East: -60.5	East: -69

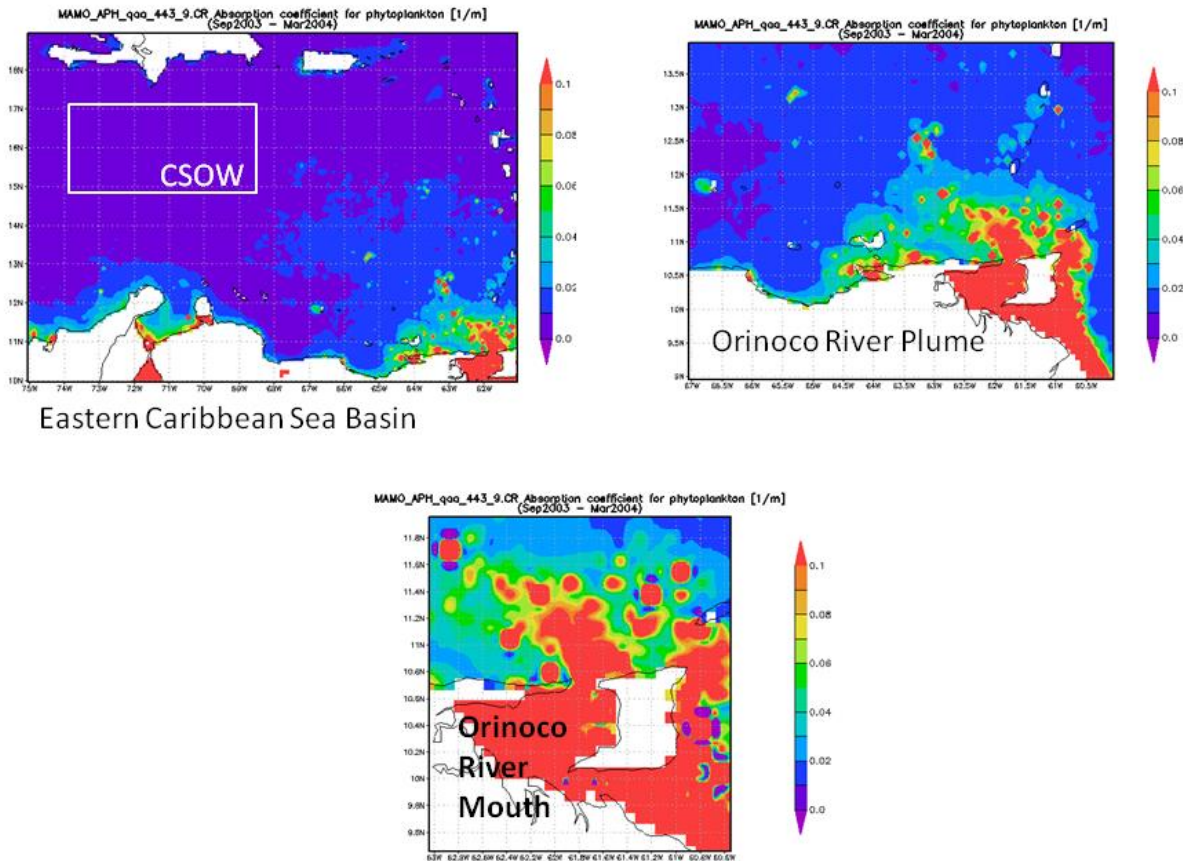


Figure 9. Area maps showing the regions used for Tri-plot analysis, depicted with maps of a_{ph} during the dry season. Each map encompasses the entire area used. (Upper left) Eastern Caribbean Sea Basin region, with the Caribbean Sea Oligotrophic Waters region (CSOW) shown by the white rectangle. (Upper right) Orinoco River Plume region. (Lower) Orinoco River Mouth region. The actual mouth of the Orinoco River, just south of the region shown, was excluded due to the large number of “no data” pixels caused by the high sediment load, which is interpreted as land.

Two time periods were selected for analysis, corresponding to the wet (rainy) and dry season in tropical South America. The wet season data were averaged for the period April-August 2013. The dry season data were averaged from September 2013 - March, 2014. This resulted in a total of eight different Triplot graphs generated – each of the four areas during the wet season and during the dry season.

3.2 Data Download Format

After selecting the three data parameters and the generation of the area average map for each parameter over the selected time period, the data are downloaded for use in Tri-plot. The data are downloaded in ASCII text format in “Batch” mode. This procedure provides output files as on-the-fly *.tar* files, which are then unzipped for use as text data input to Tri-plot.

3.3 Preparing ASCII text data for Tri-plot Analysis

After downloading the data as text values, functions and formulas in the Excel spreadsheet are used to prepare the parameter values for input into Tri-plot. The Tri-plot application requires an input of three parameters represented as percentages. Thus, the values in each row, which in this method represent the map pixel values of each parameter, will sum to 100%.

Data for each parameter in the output text file are first copied into Excel. The data are parsed into separate columns by selecting “Text to Columns” under the Data Tab. (If using the Tri-plot template, the macro “parse” will do this automatically.)

The data will be parsed into three columns: latitude, longitude, and the data parameter value. The number “-3.27670e+04” represents “no data”, primarily representing land pixels.

Following the Tri-plot template, latitude and longitude data are copied into the corresponding columns on the ‘Combined_Value’ sheet. Next, the values of the three parameters are copied into the “Raw Data” columns.

A ‘Clean Data’ column contains several formulas to replace the “-3.27670e+04” value representing “no data” with “-99” as the new “no data” value. Subsequently, the b_{bp} value is multiplied by a factor of 10, to be of similar magnitude to the values of a_{ph} and a_{dg} . If any value is less than zero, but not the “no data” value, then the value is replaced with .000001, since the percentages will not be properly calculated with negative values.

Once the raw data is entered in the columns, the percentages for the three-component system are calculated by summing, then calculating the contribution of each parameter as a percentage of the sum, as in the example for a_{dg} (Equation 1).

$$\% a_{dg} = [a_{dg} / a_{dg} + a_{ph} + (10 \times b_{bp})] \times 100 \quad (1)$$

If one cell in the row contains “no data”, the remaining parameter values are then replaced with “-99”. Further, subtracting the sum of the other two parameters from 100 generates the final b_{bp} percentage. This guarantees that all three columns sum to exactly 100, but may alter the b_{bp} value by an insignificant amount. To filter out the “no data” values from the entire list, an advanced filter with a condition (if $ADG\% > -99$) is employed. The remaining values that meet the criteria are copied to a new column, “Without “no data.” ”

3.4 Tri-plot Analysis of “Clean Data” Values

For this study, the ‘Size’ plot of the Triplot spreadsheet was used. The ‘Clean Data’ that has been calculated (the percentages of the three parameters) are entered in the “data entry area” under “proportion in class (%)” on the Tri-plot spreadsheet. Initially, the Tri-plot spreadsheet is set up for a maximum of two hundred input values. To increase this range, the formulas in the computational columns under “graph co-ordinates” are expanded to match the number of input values. If the ($b_{bp} \times 10$) value was much larger than the values for a_{dg} and a_{ph} , the calculated b_{bp} contribution was 100%, and the application attempted to plot these points along the bottom boundary of the ternary diagram.

4. Conclusions

Modern data systems and data archives have made it relatively simple to access a wide variety of remotely-sensed data products online. The NASA Giovanni system allows users to visualize and acquire numerous remotely-sensed oceanographic data variables. The availability of IOPs from MODIS-Aqua in Giovanni makes these advanced ocean optical parameters accessible to users in many different disciplines and settings, ranging from research scientists and water quality or environmental quality professional scientists to professors, teachers, students and citizen scientists. Heretofore, however, the use of IOPs has been primarily for the purpose of basic research in ocean optics. One of the limiting factors for the application of optical water mass classification was the absence of a method to make use of the IOPs without considerable effort.

The optical water mass classification system described in this paper provides a simple method to make use of the IOPs available in the NASA data product suite. The example of the Orinoco River outflow in the eastern Caribbean Sea demonstrates the use of this method and the insight it provides regarding influences on surface ocean optical properties. The contrast between dry and wet season conditions in the eastern Caribbean Sea is observable in the ternary diagrams produced by Tri-plot, as described in the Results and Discussion section. This example only demonstrates a preliminary analysis of the data; deeper statistical analyses, perhaps with more rigorous criteria for water mass classification, could be accomplished with the same data. Furthermore, analysis of multiple years would help to delineate the range of seasonal variability in the data.

The Giovanni – Tri-plot optical water mass classification method provides a way to visualize relationships between the IOPs that indicate the optically active absorbing and scattering constituents in surface waters. The method thus allows further insight into optical properties of surface waters beyond the commonly-used variables such as chlorophyll *a* concentration and diffuse attenuation coefficient at 490 nm (K490). As the Giovanni system provides global ocean optical data variables, the method described here can be applied in several investigative scenarios, ranging from the local level to monitor estuaries and rivers, to regional analyses of coastal waters and large lakes, up to and including basin-scale oceanography. The ability to produce visual ternary diagrams for optical water mass classification can thus become an additional useful analytical tool.

Acknowledgments

Analyses and visualizations used in this paper were produced with the Giovanni online data system, developed and maintained by the NASA GES DISC. Ocean color radiometry data are acquired from the Ocean Biology Processing Group at NASA Goddard Space Flight Center. Comments by Dr. Richard W. Gould and Bryn Douds enabled significant improvements to the clarity of the text.

Author Contributions

James G. Acker 55%, Erik Douuds 45%

Conflicts of Interest

The authors declare no conflict of interest.

References and Notes

1. Jerlov, N.G. Optical studies of ocean water. *Reports of the Swedish Deep-Sea Expeditions* **1951**, 3, 1-59.
2. Jerlov, N. Optical Oceanography. *Oceanography and Marine Biology Annual Review* **1963**, 1, 89-114.
3. Jerlov, N.G. *Marine Optics*. Elsevier, Amsterdam, The Netherlands, **1976**, 231 pp.
4. Morel, A.; L. Prieur. Analysis of variations in ocean color. *Limnol. Oceanogr.* **1977**, 22(4), 709-722.
5. Maritorena S.; Siegel, D.A.; Peterson, A. Optimization of a semi-analytical ocean color model for global scale applications. *Applied Optics* **2002**, 41(15), 2705-2714.
6. Lee, Z; Carder., K.L.; Arnone., R.A. Deriving inherent optical properties from water color: a multiband quasi-analytical algorithm for optically deep waters. *Applied Optics* **2002**, 41(27), 5755-5772.
7. Hoge, F.E.; Lyon, P.E.; Satellite observation of chromophoric dissolved organic matter (CDOM) variability in the wake of hurricanes and typhoons. *Geophysical Research Letters* **2002**, 29(19), 4 pages.
8. Acker, J.; Lyon, P.; Hoge, F.; Shen, S.; Roffer, M.; Gawlikowski, G. Interaction of Hurricane Katrina with optically complex water in the Gulf of Mexico: interpretation using satellite-derived inherent optical properties and chlorophyll concentration. *IEEE Geoscience and Remote Sensing Letters* **2009**, 6 (2), 209-213.
9. Arnone, R.A.; Wood, A.M.; Gould, R.W. Jr. The evolution of optical water mass classification. *Oceanography* **2004**, 17(2), 14-15.
10. Gould, R.W., Jr.; Arnone, R.A. Optical water mass classification for ocean color imagery. In *Proceedings: Current Problems in Optics Of Natural Waters*, Second International Conference, I. Levin and G. Gilbert, Eds., St. Petersburg, Russia, **2003**.
11. Gould, R.W., Jr.; Lewis, M.D.; Smith, R.D.; and Ko, D.S. Mapping coastal hypoxia in the northern Gulf of Mexico with ocean color imagery. In *Proceedings, Ocean Optics XX*, Anchorage, Alaska, 27 September -1 October, **2010**.

12. Deng, J.; Shen, H.; Xu, Z.; Ma, Z.; Zhao, Q.; and Li, C. Dynamic elastic properties of the Wufeng–Longmaxi formation shale in the southeast margin of the Sichuan Basin. *Journal of Geophysics and Engineering* **2014**, *11*, 11 pages.
13. Graham, D.J.; Midgley, N.G. Graphical representation of particle shape using triangular diagrams: an Excel spreadsheet method. *Earth Surface Processes and Landforms* **2000**, *25(13)*, 1473-1477.
14. Method note: For Giovanni to generate data values that can be directly placed in the Excel spreadsheet, the “Parameter Max” value for b_{bp} must be manually set to .01 instead of 0.1, due to parameter scaling of the output value by Giovanni. This is accomplished using the “Edit Preferences” feature in Giovanni.

© 2015 by the authors; licensee MDPI, Basel, Switzerland. This article is an open access article distributed under the terms and conditions of the Creative Commons Attribution license (<http://creativecommons.org/licenses/by/4.0/>).